Week 7

Bonding in Coordination Complexes

7.1   Coordination Complexes: π Bonding and all-σ Distortions

11/7: • Video lecture Wed and Fri; watch by Mon and have questions.

- Last time: MO diagram for an ML_6 coordination complex whose ligands only engage in σ interactions.

- Today: The case where the ligands also have π orbitals.

- As per usual, we follow the procedure from Lecture 6.1.

  1. Point group: O_h.
  2. Assigning coordinate axes is a bit more complicated here, but the following will work.
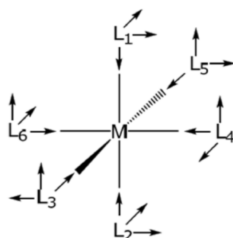

Figure 7.1: ML_6 π xyz coordinates.

  - We have two orthogonal $p\pi$ bonds.
  - The arrows indicate the directional phase of the p orbitals.
  3. Let's create a representation for the 12 p orbitals capable of π bonding.

O_h	E	$8C_3$	$6C_2$	$6C_4$	$3C_2$	i	$6S_4$	$8S_6$	$3\sigma_h$	$6\sigma_d$
$\Gamma_{12\pi}$	12	0	0	0	-4	0	0	0	0	0

Table 7.1: Representation for the $p\pi$ ligand orbitals of ML_6.

  4. Reducing, we get
$$\Gamma_{12\pi} = T_{1g} + T_{1u} + T_{2g} + T_{2u}$$
  5. From Table 6.8, the atomic orbitals of the metal transform as

$$s \sim a_{1g} \qquad p_x, p_y, p_z \sim t_{1u} \qquad d_{z^2}, d_{x^2-y^2} \sim e_g \qquad d_{xz}, d_{yz}, d_{xy} \sim t_{2g}$$

  - Thus, the metal p and d_{xz}, d_{yz}, d_{xy} orbitals interact with the ligand π SALCS.

6. Once again, we can "guess" the SALCs based on experience.

(a) t_{1u} bonding.   (b) t_{2g} bonding.   (c) t_{1g} nonbonding.   (d) t_{2u} nonbonding.
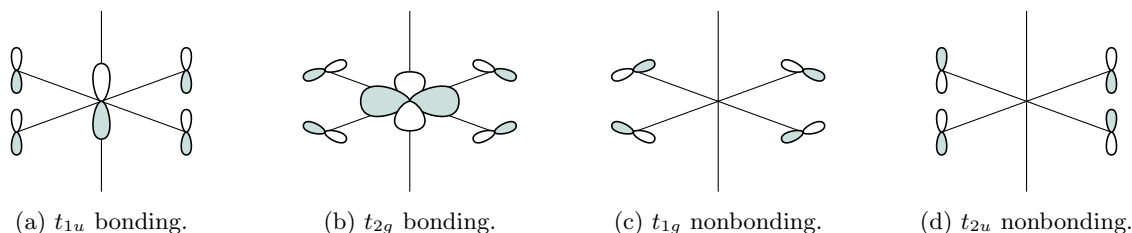
Figure 7.2: ML_6 π SALCs.

– In addition to these, there are two more (oriented along the other orthogonal coordinate axes) for each IRR.
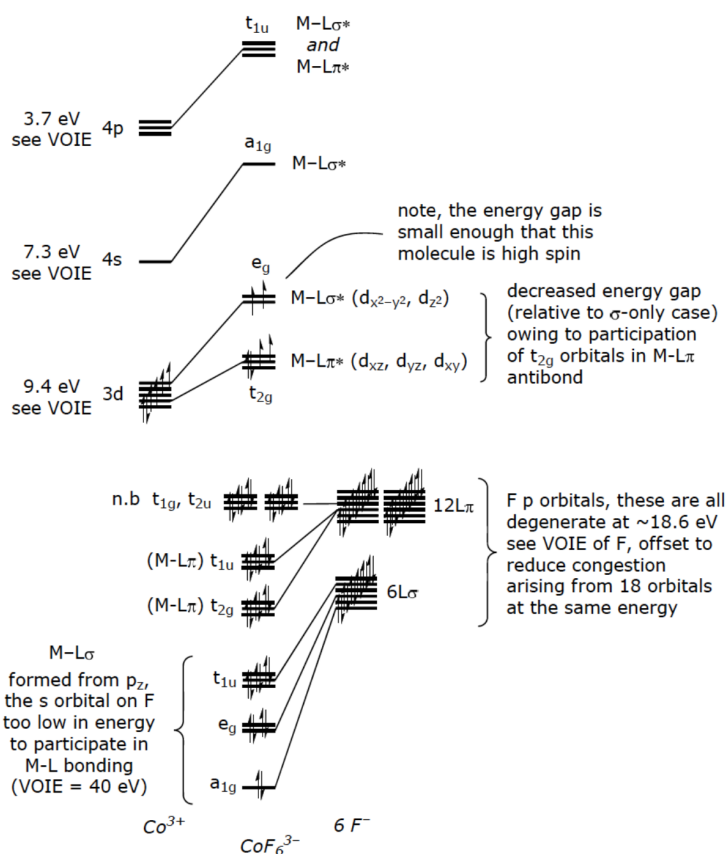
7. We can now make sense of the MO diagram.

Figure 7.3: ML_6 π MO diagram.

– Wuttig compares this MO diagram to the all-σ case (Figure 6.13).
  ■ The M-Lσ and M-Lσ^* distortions stay the same; we now just have *additional* M-Lπ and M-Lπ^* distortions to consider.
  ■ π-donating ligands, such as the fluoride ligands causing the interactions in Figure 7.3, *raise* the t_{2g} set in energy; they contribute *antibonding* interactions.
  ■ Note that the Lπ orbitals sit above the Lσ orbitals.
– Wuttig probably expects us to be familiar with the M-Lπ^* notation.

- It seems that now we're done. But wait: We have made an assumption that is not necessarily justified in every case.

  – We have treated the ligand as a point particle with atomic orbitals that mirror the metal center (i.e., your typical s, p, etc. orbitals).

  – This is justified in the case of fluoride (as in Figure 7.3). But what about a ligand such as carbon monoxide? CO certainly has molecular orbitals more complicated than the atomic orbitals of either carbon or oxygen alone, so is it still valid to treat it as a point particle with "atomic" orbitals?

  – In fact, it is not, and we will now see how to treat that case.

- As with fluoride, the frontier orbitals of CO will be the ones that interact with the metal center.

- To draw SALCs of the interactions of these MOs with the metal center, we need to know what *they* look like first. Fortunately, we have encountered the SALCs for heteronuclear diatomics before, and we can simply use these as our basis set to draw the overall SALCs.

(a) t_{1u} bonding.   (b) t_{2g} bonding.
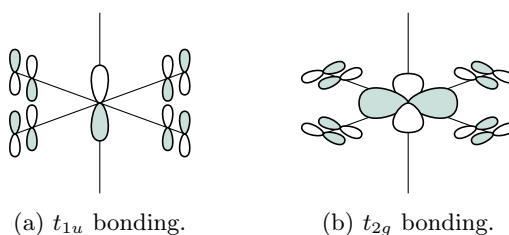
Figure 7.4: $M(CO)_6$ π-bonding SALCs.

  – Wuttig draws the Figure 7.4a interactions in-plane, too, though??

  – Wuttig also doesn't draw the nonbonding ones, but they still exist??

  – To reiterate, the π^* orbitals of CO will participate in t_{1u} and t_{2g} bonding interactions, and t_{1g} and t_{2u} nonbonding interactions just like the p orbitals of F; it is *strictly* and *solely* the basis set that we're changing.

- An additional complication arises from the fact that the frontier orbitals of CO are fundamentally different than those of F.

  – In particular, the frontier orbitals of F are filled π-donating atomic orbitals, while CO has a filled σ-donating frontier orbital (HOMO) and an unfilled π^*-accepting frontier orbital (LUMO).

  – Thus, we need to consider the new *energetics* of these orbitals as well.

  – For a π-donating ligand such as monoatomic fluoride, the σ and π orbitals are degenerate.

    ■ This is because all 18 ligand orbitals come from the $2p$ *atomic* orbitals of fluorine.

  – However. . .

- Are the σ and π orbitals of the π-accepting ligands degenerate in energy?

  – They are not.

  – This is because we are considering the interactions of nondegenerate ligand *molecular* orbitals with the metal center.

  – Evidence: We can inspect the photoelectron spectrum of our ligand (e.g., for CO, we observe distinct peaks corresponding to its σ-donating and π^*-accepting orbitals).

  – Note that ligands such as CO still have filled π MOs; it's just that these lie so low in energy that they don't interact with the metal center.

- The consequence of this is that the π ligand orbitals of a π-accepting ligand lie significantly higher in energy.

  - In fact, they lie higher in energy than a metal's d orbitals, meaning that the metal t_{2g} set is now M-Lπ *bonding* instead of *antibonding* and hence lower in energy, leading to a greater d orbital splitting.

- All of this can be summarized by the MO diagram for a ML$_6$ complex with π-accepting ligands.
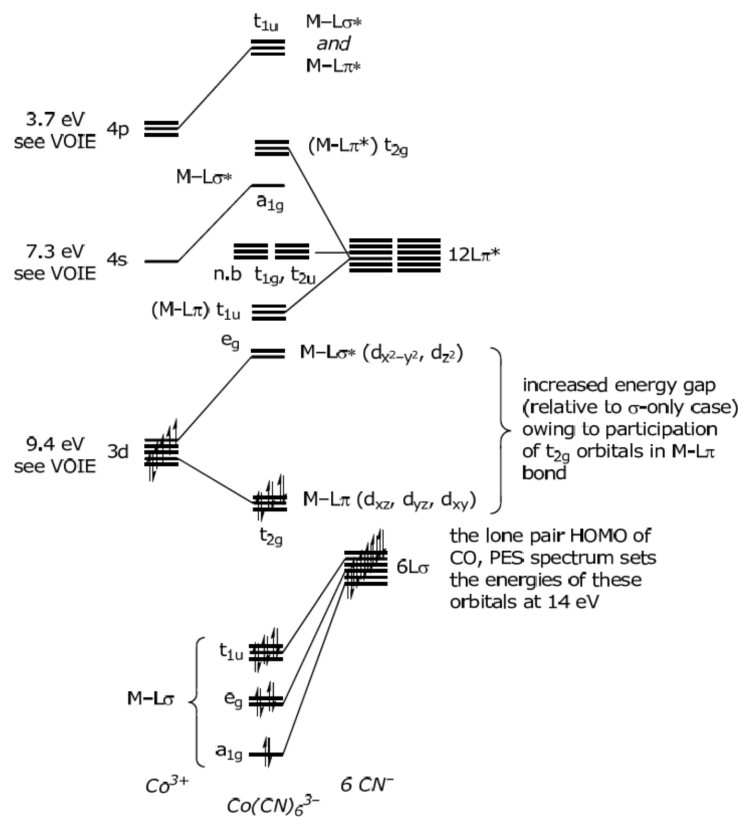
Figure 7.5: ML$_6$ π-accepting MO diagram.

- Distortions from σ interactions.

- Consider a ML$_6$ complex with σ-only interactions, as discussed last class.

  - Goal: Predict Jahn-Teller distortions from first principles.
  - Two possible distortions: A tetragonal compression or a Jahn-Teller elongation.
    - See Figure VI.10 of Labalme (2022).
    - Are both of these distortions not "Jahn-Teller" effects??
  - Either distortion changes the point group from O_h to D_{4h}.

- We now seek to build an MO diagram for the t_{2g} and e_g set of each distortion.

  - To begin, we determine the symmetries are the d orbitals in the two point groups (see Table 7.2).
  - Since the t_{2g} set is nonbonding in a σ-only complex, their energy doesn't change much, so the distorted t_{2g} set is basically still degenerate. However, we do have to draw the b_{2g} MO slightly higher (or lower, but we choose higher) since it has a different symmetry.

	O_h	D_{4h}
$d_{x^2-y^2}$	e_g	b_{1g}
d_{z^2}	e_g	a_{1g}
d_{xy}	t_{2g}	b_{2g}
d_{yz}	t_{2g}	e_g
d_{xz}	t_{2g}	e_g

Table 7.2: d-orbital symmetries in O_h vs. D_{4h}.

– The e_g orbitals definitively split, going in different directions as the axial ligands compress or expand. In particular, compressing the axial ligands drives d_{z^2} up (and $d_{x^2-y^2}$ down), and vice versa for expanding the axial ligands.

– Note that the original e_g set is M-Lσ^*, which is why compression drives up energy (more mixing between regions of opposite phases is not energetically favorable).